JOURNAL OF OPTOELECTRONICS AND ADVANCED MATERIALS Vol. 12, No. 9, September 2010, p. 1969 - 1975

Heterocyclic azodyes as pigments for dye sensitized solar cells – A combined experimental and theoretical study

J. LUNGU[a], C.I. OPREA[a], A. DUMBRAVĂ[b], I. ENACHE[b,c], A. GEORGESCU[a], C. RĂDULESCU[d], I. IONIȚĂ[d]
G.V. CIMPOCA[d], M. A. GÎRȚU[a*]
[a]*Department of Physics, Ovidius University of Constanța, Constanța 900527, Romania*
[b]*Department of Chemistry, Ovidius University of Constanța, Constanța 900527, Romania*
[c]*Department of Mathematics and Sciences, Constanța Maritime University, Constanța 900663 Romania*
[d]*Department of Sciences, Valahia University, Târgovişte 130024, Romania*

We report the results of a combined experimental and theoretical study of four azodyes, derived from three different heterocyclic systems, which we used as sensitizers for TiO_2 dye-sensitized solar cells. Although the efficiencies are relatively low, of up to 0.19%, the fill factors are competitive, with values of up to 0.74. To better understand the large differences in the overall photovoltaic conversion efficiency between the four dyes we performed DFT calculations to determine the energy levels of the ground and excited states of the pigments. We explain the experimental results based on the energy level alignment with respect to the TiO_2 substrate and the electrolyte.

(Received August 2, 2010; accepted September 15, 2010)

Keywords: Dye-sensitized solar cells, Photovoltaic conversion efficiency, TiO_2, azodyes, Density functional theory

1. Introduction

Among third generation photovoltaic devices [1], dye-sensitized solar cells (DSSCs) [2] have attracted a special interest due to the prospect of low production cost [3], transparency and flexibility, when desired. For such reasons, DSSCs may constitute a choice for affordable power generation in niche markets, particularly for producing power generating windows [4].

Dye Sensitized Solar Cells are photovoltaic devices based on the photosenzitation of a porous layer of nanocrystalline wide band gap semiconductor, such as anatase TiO_2, with a light absorbing pigment. The DSSCs consist of a dye-sensitized electrode, a redox electrolyte (e.g. I_3^-/I^-) and a counter electrode for instance platinized conductive glass. The working principle of the device is based on light absorption in the dye anchored to the TiO_2 nanocrystal. The resulting photoelectron is transferred from the excited level of the dye into the conduction band of TiO_2, and through the electrode into the external circuit. The sensitizer is restored by electron donation from the iodide ion, which is regenerated in turn by reduction of the triiodide ion at the counter electrode [2].

The efficiency of the photovoltaic device depends strongly upon the dye used. The highest efficiencies of power conversion in standard air mass 1.5 global (AM 1.5G) conditions, obtained for metal free dyes reach values of up to 9% [5]. Although the efficiency of the metal-free dyes is lower than that of the typical Ru-based dyes [2], they possess some advantages such as the ease of synthesis, high molar extinction coefficient, tunable absorption spectral response from the visible to the near infrared region, as well as environmentally friendly and low cost production methods [6].

In the search for new dyes for DSSCs, much attention has been given to natural pigments [7] or synthetic metal-free organic dyes such as merocyanines, coumarins, styryl, indoline dyes, ring fluorinated fluoresceins [8], organic dyes with triethoxysilyl units as anchoring groups [9], and recently, to synthetic textile mordant dyes, most of them based on the azo (–N=N–) group [10]. The azodyes benefit from a relatively intense absorption in the visible region ant the absence of heavy metals [11].

We report here on the fabrication and characterization of DSSCs using as pigments four azodyes derived from three different heterocyclic systems. To better understand the results of our electro-optic experimental studies we performed Density Functional Theory (DFT) calculations providing the geometry optimization and the electronic structure of the dyes. Based on an analysis proposed by another group [12] and refined by us [11] we compare the molecular energy levels of the dyes to the band edges of the oxide and the redox level of the electrolyte. Thus, we are able to discuss the importance of various requirements for the sensitizing pigments in order to design higher efficiency solar cells.

2. Experimental

2.1. Solar cell fabrication and testing

We used as DSSC pigments four azodyes, all derived from three different heterocyclic systems [13]. More precisely, the first pigment, dye **1**, was based on 2-aminothiazolo[4,5-b]quinoxaline-6-carboxylic acid, dye **2** on 2-aminothiazolo[4,5-b]pyridine, dyes **3** and **4** on 2-aminothiazolo[4,5-f]indazole [13], as shown in Fig. 1.

The photoelectrodes were prepared by covering with a TiO_2 paste the conductive glass substrates, following a pretreatment in a $TiCl_4$ 0.2M solution, for 40 min at 70 ^oC (to increase the short-circuit photocurrent [14]).

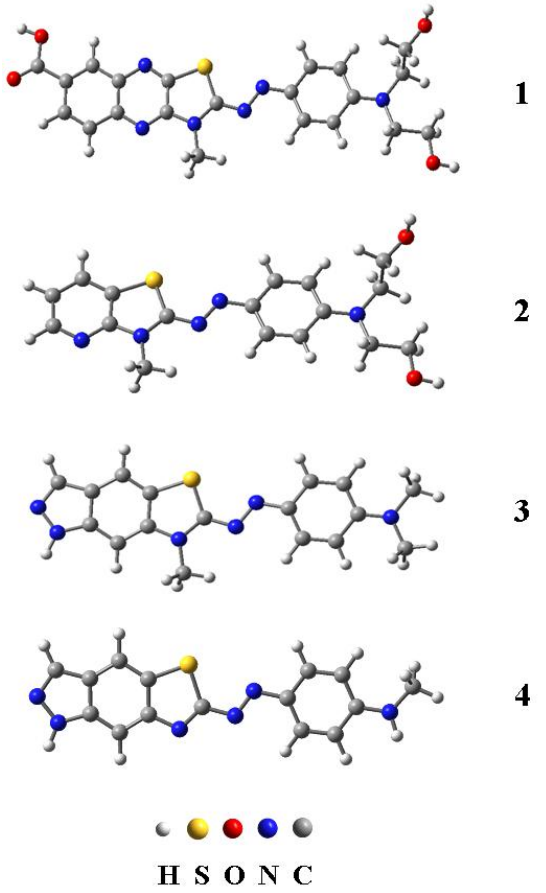

*Fig. 1. Azodyes derived from heterocyclic systems: (**1**) is based on -aminothiazolo[4,5-b]quinoxaline-6-carboxylic acid, (**2**) on 2-aminothiazolo[4,5-b]pyridine, (**3**) and (**4**) on 2-aminothiazolo[4,5-f]indazole.*

The TiO_2 paste was obtained starting from a polyester-based titanium sol, which was mixed with nanocrystalline anatase TiO_2 powder (P25, Sigma-Aldrich) in proper molar ratio [15]. The paste was applied onto the pretreated soda lime glass sheet of 2.2 mm thickness, covered with a conductive layer of fluorine-doped tin oxide (SnO_2:F) with a 7 ohm/square resistivity (Solaronix), by the "doctor-blade" technique. After the coating with the porous film of TiO_2, the photoelectrodes were sintered at 450^0C for 1h in an oven. For post-treatment, the photoelectrode was kept in a $TiCl_4$ 0.2M solution, overnight at room temperature, and than in an oven at 450^oC for 1h. The final step in the preparation of the photoelectrode consisted in immersion in the pigment solutions for 2 h at 80^0C. Afterwards, the plates were rinsed in water until the rinse liquid was colorless, dried at 80 ^oC.

Platinum counter electrodes were prepared by spreading a few drops of 5mM $H_2[PtCl_6]\cdot 6H_2O$ solution in 2-propanol onto the conductive glass, followed by drying at 100ºC for 10 min and than at 400ºC for 30 min.

The electrolyte liquid (Iodolyte TG-50, Solaronix) is drawn into the space between the electrodes by capillary action. To assembly the DSSCs the plates were secured together with small bulldog clips [10,16].

The UV-VIS absorption spectra of dye aqueous solutions and dyes adsorbed on TiO_2 surface were recorded in the range 200 – 900 nm and 220 – 850 nm, respectively, with a Jasco V 550 spectrometer, either in quartz cuvettes in absorption mode or in an integrating sphere. The electro-optic parameters of the DSSCs, mainly the fill factor, *FF*, the photovoltaic conversion efficiency, η, the short circuit current, I_{SC}, and the open circuit voltage, V_{OC}, of the photovoltaic cells were measured under AM 1.5G standard sun conditions ($1000W/m^2$) at 25^oC, using a class A small area solar simulator [17]. The cell surface was exposed to light through a circular slit of 10 mm diameter, resulting in a useful area of about 0.785 cm^2. The current and voltage values were measured using two digital bench multimeters (Mastech MS8050) and a precision decadic resistance box. All measurements were made at about 45 s intervals, allowing time for each reading to stabilize.

2.2. Computational details

The ground state geometrical structures of the dyes were optimized using Density Functional Theory (DFT) methods [18] with the hybrid B3LYP exchange- correlation functional [19] and the double-ζ quality basis functions for valence electrons with polarization functions (DGDZVP [20]). Optical absorption spectra of all complexes, including the lowest 20 singlet-singlet excitations, were simulated using the Time Dependent-DFT (TD-DFT) method [21] with the same functional and basis set. The spectral lines were convoluted with Gaussian distributions of 20 nm linewidth at half maximum. Solvent effects in water were accounted for by employing the non-equilibrium conductor-like polarizable continuum model (C-PCM) [22]. All calculations were performed with the GAUSSIAN03 package [23].

3. Results and discussion

The experimental UV-Vis spectra of the four dyes in aqueous solutions and adsorbed onto the TiO_2 layer of the photoelectrode, as well as the theoretical electronic spectra calculated for all dyes and their corresponding deprotonated (**1** and **2**) or protonated (**4**) forms are shown in Fig. 2. It can be seen that both the experimental and the theoretical UV-Vis spectra show strong absorption in the visible range for all dyes.

In the case of dye **1** the spectrum has a broad maximum at 584 nm for a solution of pH = 7. A maximum at about the same wavelength is obtained for the dye adsorbed on the substrate. The low intensity of the band can be correlated not only with the differences between the two types of measurement (transmission and reflectance) but also with a relatively poor adsorption on the TiO_2 layer, observed experimentally when visually examining the photoanode.

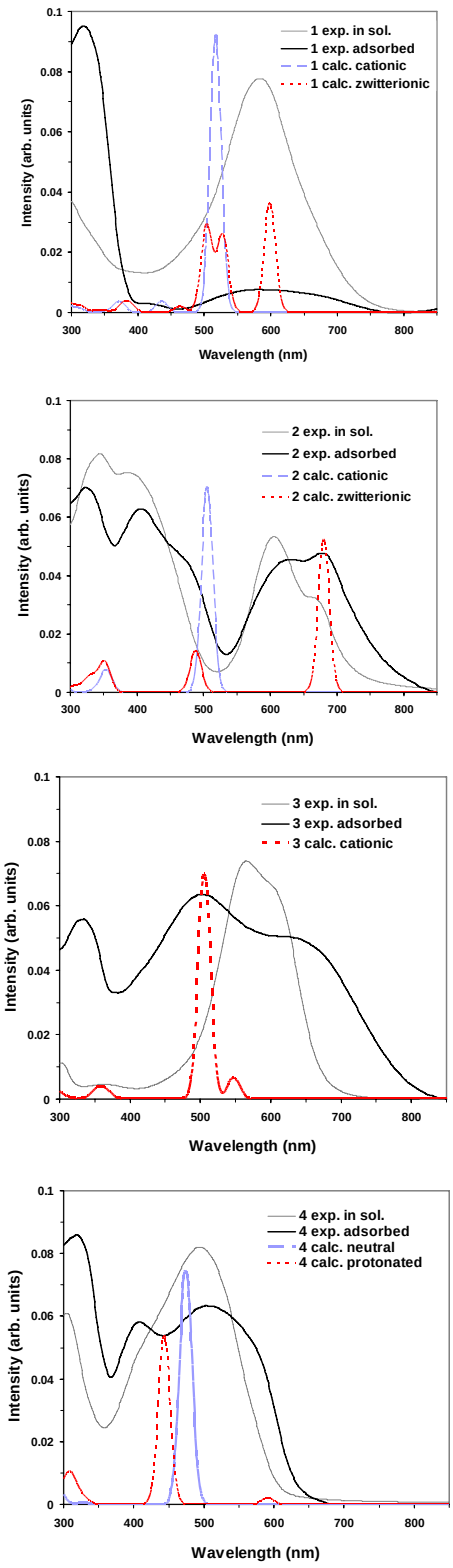

Fig. 2. Experimental UV-Vis spectra in solution and adsorbed onto the TiO_2 layer of the photoelectrode, together with the theoretical electronic spectra calculated for protonated and/or deprotonated dyes. The theoretical spectra were obtained using convolutions of Gaussian distributions with a full width at half maximum of 20 nm.

The calculated electronic spectrum of the dye shows a strong peak at 517 nm in the case of the cationic dye. Calculations of the deprotonated, zwitterionic form of **1**, lead to a spectrum with two transitions at 504 and 527 nm and a more intense one at 599 nm. Convoluting these three absorption bands using wider Gaussians we find a better agreement between the calculations performed on the zwitterionic form of the dye and the experimental data for the adsorbed pigment. Although the deprotonation process is chemically unlikely for the cation in solution of neutral pH [24], on the TiO_2 substrate the deprotonation is probable [25].

For dye **2** although qualitatively similar, with two features at 325 and 406 nm and then at 629 and 678 nm, quantitatively, the two experimental spectra are different, with broader band, extending into the IR for the adsorbed dye. The differences between the two experimental spectra may be due to the interaction with the substrate. Despite the lack of –COOH groups, the dye binds to the TiO_2 layer and extends the absorption bands to higher wavelengths. The calculated spectra in the visible range show a single transition (at 505 nm) for the cationic dye **2** and two transitions (at 488 nm and 680 nm) for the deprotonated, zwitterionic form of **2**, which resulted after extracting a H atom from the -OH group closest to the plane of the rings. Again, based on the number and position of peaks we notice a better agreement between the experimental data and the results of the theoretical calculations for the deprotonated, zwitterionic form of the dye. The arguments mentioned for **1** are even stronger in the case of **2**, as the binding to the substrate is stronger. Even though the deprotonation of the cation is unlikely in solution of neutral pH [24], it is probable when adsorbed onto the TiO_2 substrate [25,26].

The UV-Vis experimental spectra for dye **3** reveal larger discrepancies. We note here that the dye had very poor adherence to the substrate, revealed when rinsing the photoelectrode, as most of the dye would be washed away. The observation was not surprising as the dye lacks anchors to attach itself to the oxide [2,25].

Dye **4** is soluble only in low pH aqueous solutions, which makes possible the protonation of the dye. The experimental spectra have some qualitative similarities, both with a feature at ~410 nm and at ~505 nm. The theoretical spectra for the neutral dye has just one transition in the visible range, at 474 nm, whereas for the dye in the protonated form we obtained an intense transition at lower wavelengths, 444 nm, and a very weak one at 591 nm.

The *I-V* curves for some typical DSSCs fabricated with dyes **1**, **2** and **4** (as we mentioned above, dye **3** was not appropriate for the production of solar cells) are shown in Fig. 3. We first note that dyes **2** and **4** display clear photovoltaic behaviour, whereas dye **1** shows invariably poor conversion of visible light into electricity. The values of the electro-optic parameters of the typical DSSCs fabricated are displayed in Table 1.

The shape of the *I-V* curve for the cells based on dye **2** is clearly the closest to what we expect from a photovoltaic cell. The high fill factor of 0.74 is comparable to that of typical first generation solar cells based on silicon devices [1]. The cell based on dye **4** provides the highest current

but has poor fill factor and efficiency. Although the photovoltaic conversion efficiency is low, the value obtained for dye **2** compares well to other metal-free dyes and natural pigments [7-10].

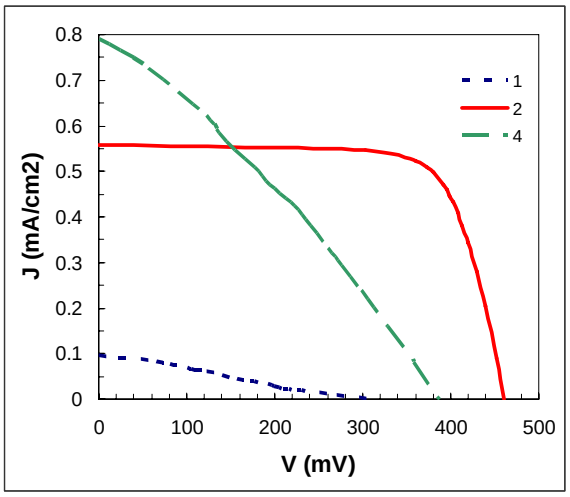

*Fig. 3. Current-voltage curves for typical dye-sensitized solar cells fabricated with dyes **1**, **2** and **4**, measured under standard illumination conditions.*

Table 1. Electric parameters (short circuit current, I_{SC}, open circuit voltage, V_{OC}, fill factor, FF, photovoltaic conversion efficiency, η) of typical DSSCs measured under standard illumination conditions (see also Fig. 3).

Dye	I_{sc} (mA/cm^2)	V_{oc} (mV)	P_{max} (mW)	*FF*	η (%)
1	0.074	305	5.658	0.25	0.0072
2	0.438	461	149.2	0.74	0.1901
4	0.62	387	74.12	0.31	0.0944

These results are to some extent puzzling, as the carboxyl and/or hydroxyl groups at the periphery of **1** and **2** favour the adsorption on the substrate, thus making them better candidates as pigments for DSSCs than **3** and **4**. To better understand our experimental results we performed DFT calculations providing the geometry optimization and the electronic structure of the dyes. The energy of the highest occupied (HOMO) and the lowest unoccupied (LUMO) molecular orbitals of the dyes, together with the energies of the valence (VB) and conduction (CB) band edges for TiO_2 [12] and the redox level of the I_3^-/I^- electrolyte [2,27] are displayed in Fig. 4. The values on the axes in Fig. 4 are relative to the vacuum (on the left axis) and to the normal hydrogen electrode (NHE, on the right axis) [11]. The doted lines are drawn as aids to the eye for an easier examination of the energy level alignment.

Regarding dye **1**, the obvious remark is that the LUMO lies well below the conduction band edge of TiO_2 in both cationic and zwitterionic forms, making very unlikely the transfer of the photoelectron from the dye to the semiconducting oxide. This theoretical result together with the weak absorption in the visible range and poor adsorption onto the substrate observed experimentally during the optical measurements and device fabrication, explain the extremely low efficiency of the DSSCs based on **1** and the poor shape of the *I-V* curve.

In the same way, for **2** in the cationic form the excited state of the dye is located below the CB edge by about 0.3 eV. However, in the deprotonated, zwitterionic form, dye **2** displays a relatively good energy alignment between the LUMO and the CB. Moreover, the same good alignment occurs between the HOMO and the redox level of the electrolyte. Therefore, the experimental results showing the highest efficiency for **2** are consistent with the calculated energies for the deprotonated form, and in agreement with the better correspondence between the experimental and calculated optical spectra. However, the low value compared to the best DSSCs reported in the literature [28] is likely due to the weak absorption in the green region of the spectrum.

In the case of **3** the main problem was the lack of adherence of the dye to the TiO_2 layer. However, even if the pigment had been adsorbed onto the substrate, it would have shown a very low efficiency due to the improper alignment between the LUMO of **3** and the CB edge of the oxide.

Pigment **4** in its neutral form also shows relatively good energy alignments, in agreement with the efficiency obtained experimentally. Noting that the HOMO lies deeper below the redox level and the LUMO higher than the CB, while the absorption spectrum is slightly better matched with the solar spectrum, it is not obvious, with simple arguments, why the efficiency is so low compared to that of dye **2**. The poorer binding to the oxide may be one of the causes. Another possibility may arise from the lower V_{oc} value, which may be due to the lowering of the CB edge in a solution with low pH, as reported by other authors [29].

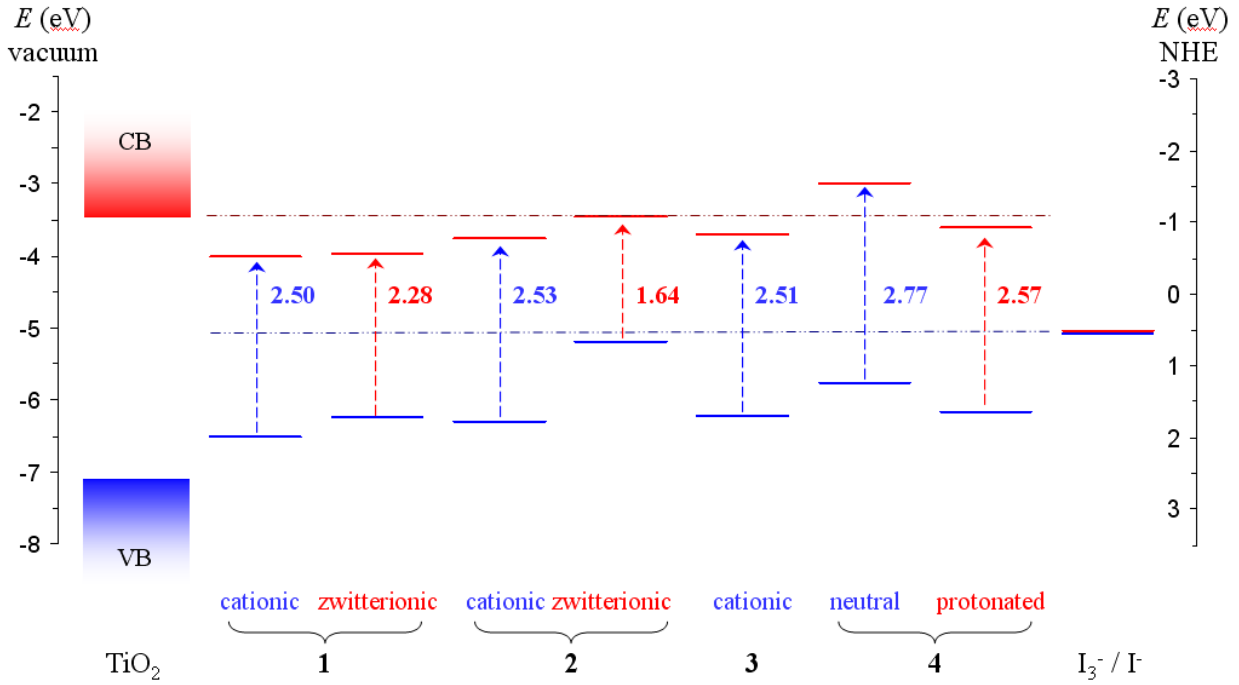

Fig. 4. Energy diagram showing the CB and VB edges of the TiO_2 substrate [12], the HOMO and LUMO levels of the dyes **1**, **2**, **3**, *and* **4**, *and the redox potential of electrolyte [**Error! Bookmark not defined.**].*

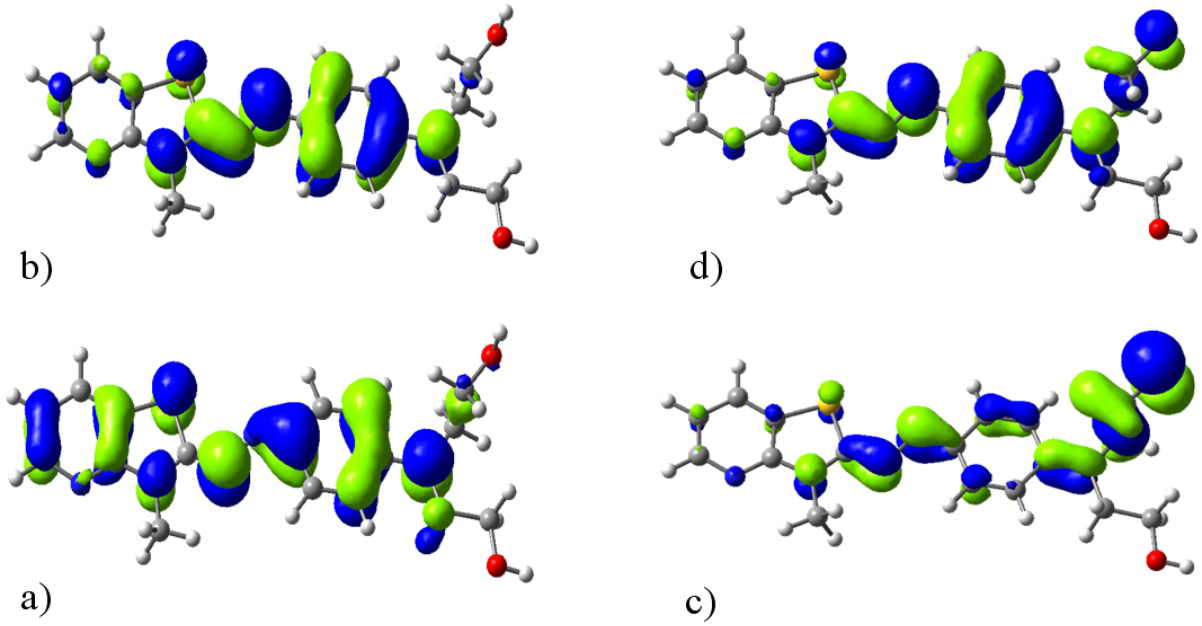

Fig. 5. Electron isodensity contours (0.03 e/a_o^3) of dye **2** *molecular orbitals: a) HOMO and b) LUMO of the cationic dye, c) HOMO and d) LUMO of the deprotonated zwitterionic form.*

In contrast, the protonated form of **4** has the LUMO below the CB edge of the oxide by 0.16 eV. In such a case, the electron transfer to the oxide is less likely. The contradiction with the observed *I-V* curve and the efficiency obtained suggests that dye **4** is more probable present in its neutral form in our DSSCs.

In closing this section it is worth to examine the nature of the orbitals, to comment on the likelihood of the charge transfer. Figure 5 displays the electron density of the most relevant molecular orbitals of dye **2**, MOs that are involved in the most intense optical transitions. It can be seen that for **2** in both the cationic and deprotonated forms the MOs have π character, the transitions from the HOMO to the LUMO is in each case a π → π* transition. The MOs of the cationic dye are delocalized over the entire molecule, whereas the orbitals of the corresponding deprotonated

pigment are more localized, with a higher density towards the deprotonated hydroxyl group, that is towards the end that likely binds to the TiO_2. Simplifying the charge transfer processes and thinking in terms of the higher orbital overlap between the π^* orbital of the dye and the crystalline orbital of the oxidic substrate, the electron injection into the semiconductor is more likely in the case of the deprotonated, zwitterionic form of dye **2**., consistent with all our other results.

5. Conclusions

We reported results of a combined experimental and theoretical study of four azodyes dyes, derived from three different heterocyclic systems based on the –N=N– group.

We fabricated and tested under standard illumination conditions DSSCs using the four dyes, nanocrystalline anatase TiO_2 and I_3^-/I^- electrolyte. We found that dyes **1**, **2**, and **4** present light harvesting properties and perform charge transfer sensitization of the TiO_2 semiconducting layer. Surprisingly, although *a priori* **1** and **2** are better candidates as pigments for DSSCs than **3** and **4** because of the carboxyl and/or hydroxyl groups at the periphery, which favour the adsorption on the substrate, the lowest current and efficiency was obtained for **1.** No photovoltaic effect was observed for **3** because of poor adsorption on the substrate. Although the efficiencies are relatively low, of up to 0.19% for **2**, the fill factors are competitive, with values of up to 0.74, again for **2**.

To better understand the large differences in the overall photovoltaic conversion efficiency between the four dyes, we performed DFT calculations to determine the energy levels of the ground and excited states of the pigments. We were able to explain the experimental results based on the energy level alignment with respect to the TiO_2 substrate and the electrolyte.

If we were to make a hierarchy of some of the main criteria required of a dye in order to be used in a DSSC, based on our study, we suggest that the first condition to be met is the proper binding to the oxide. The lack of anchoring groups that could allow the adsorption to the semiconducting substrate (such is the case for **3**) prevents any use in photovoltaic cells. The second most important criterion is, in our opinion, related to the appropriate energy level alignment between the excited state of the dye and the conduction band edge of the oxide, as well as between the ground state of the pigment and the redox level of the electrolyte. Lack of alignment (as is the case with **1**) leads to poor efficiency. The third requirement is related to the matching of the absorption spectrum with the solar irradiation spectrum. Although it has good energy level alignment, **2** still leads to a small photovoltaic conversion efficiency because of poor absorption in the green of the visible spectrum. A forth criterion is related to the electron transfer probability (once the energetics of the process are met). The transfer is more likely when the electron of the excited state of the dye is more localized towards the substrate and when the overlap between that orbital and the crystalline orbital of the TiO_2 semiconductor is high.

In conclusion, although the photovoltaic conversion efficiencies of our devices are relatively low, some of the fill factors are competitive and promising. Moreover, such studies reveal the importance of various criteria that are required of the sensitizing pigments and provide important hints in designing new dyes for higher efficiency solar cells.

Acknowledgments

C.I. Oprea acknowledges the financial support from CNCSIS/UEFISCSU grant PN2-RU-PD-603/2010. The authors thank Fanica Cimpoesu for useful discussions.

References

[1] S. E. Shaheen, D. S. Ginley, G. E. Jabbour, MRS Bulletin **30**, 10 (2005).
[2] B. O'Regan, M. Gratzel, Nature **353**, 737 (1991); M. Grätzel, Nature **414**, 338 (2001).
[3] M. Yamaguchi, Renew. Sust. Energy Rev. **5**, 113 (2001).
[4] H. Arakawa (Ed.), Recent Advances in Research and Development for Dye-Sensitized Solar Cells, CMC, 2001.
[5] S. Ito, S. M. Zakeeruddin, R. Humphry-Baker, P. Liska, R. Charvet, P. Comte, M. K. Nazeeruddin, P. Pechy, M. Takata, H. Miura, S. Uchida, M. Gratzel, Adv. Mater. **18**, 1202 (2006), D. Kuang, S. Uchida, R. Humphry-Baker, S.M. Zakeeruddin, Michael Gratzel, Angew. Chem. Int. Ed. **47,** 1923 (2008).
[6] Q. Li, L. Lu, C. Zhong, J. Huang, Q. Huang, J. Shi, X. Jin, T. Peng, J. Qin, and Z. Li, Chem. Eur. J. **15**, 9664 (2009).
[7] K. Hara, T. Sato, R.. Katoh, A. Furube, Y. Ohga, A. Shinpo, S. Suga, K. Sayama, H. Sugihara, H. Arakawa H., J. Phys. Chem. B **107**, 597 (2003); S. Ito, S.M. Zakeeruddin, R. Humphry-Baker, P. Liska, R. Charvet, P. Comte, M.K. Nazeeruddin, P. Pechy, M. Takata, H. Miura, S. Uchida, M. Gratzel, Adv. Mater. **18**, 1202 (2006); A. Dumbravă, A. Georgescu, G. Damache, C. Badea, I. Enache, C. Oprea, M.A. Gîrțu, J. Optoelectr. Adv. Mater. **10,** 2996 (2008).
[8] K. Funabiki et al., Journal of Fluorine Chemistry **127,** 257 (2006).
[9] C. Baik, D. Kim, M. S. Kang, S. O. Kang, J. Ko, M. K. Nazeeruddin, M. Grätzel, J. Photochem. Photobiol. A: Chemistry **201**, 168 (2009).
[10] K.R. Millington, K.W. Fincher, A.L. King, Sol. Energy Mater. Sol. Cells **91**, 1618 (2007).
[11] C.I. Oprea, A. Dumbravă, I. Enache, J. Lungu, A. Georgescu, F. Moscalu, C. Oprea, M.A. Gîrțu, to be published; A. Dumbravă, C.I. Oprea, I. Enache, J. Lungu, A. Georgescu, F. Cimpoesu, M.A. Gîrțu, to be published.
[12] F. de Angelis, S. Fantacci, A. Selloni, Nanotechnology **19**, 424002 (2008).

[13] C. Rădulescu, C. Tărăbăşanu-Mihailă, Revista de Chimie **55**, 25 (2004); ibid. **55,** 102 (2004); ibid. **55,** 1006 (2004).
[14] S. Ito, P. Chen, P. Comte, M.K. Nazeeruddin, P. Liska, P. Pechy, M. Gratzel, Prog. Photovolt: Res. Appl. **15**, 603 (2007).
[15] U.O. Krasovec, M. Berginc, M. Hocevar, M. Topic, Sol. Energy Mater. Sol. Cells **93**, 379 (2009).
[16] G. P. Smestad, M Gratzel, J. Chem. Educ. **75**, 752 (1998).
[17] A. Georgescu, G. Damache, M. A. Gîrţu, J. Optoelectron. Adv. Mater. **10** (2008) 2996.
[18] P. Hohenberg, W. Kohn, Phys. Rev. **136**, B864 (1964); W. Kohn, L.J. Sham, Phys. Rev. A, **140,** 1133 (1965); R. G. Parr, W. Yang, Density-Functional Theory of Atoms and Molecules (Oxford University Press, New York, 1989).
[19] A.D. Becke, J. Chem. Phys. **98,** 5648 (1993); C. Lee, W. Yang, R.G. Parr, Phys. Rev. **B 37,** 785 (1988).
[20] N. Godbout, D. R. Salahub, J. Andzelm, E. Wimmer, Can. J. C hem. **70**, 560 (1992); C. Sosa, J. Andzelm, B. C. Elkin, E. Wimmer, K. D. Dobbs, D. A. Dixon, J. Phys. Chem. **96**, 6630 (1992).
[21] E. Runge and E.K.U. Gross, Phys. Rev. Lett. **52**, 997 (1984); M.A.L. Marques, C.A. Ullrich, F. Nogueira, A. Rubio, K. Burke, and E.K.U. Gross (eds.), Time-Dependent Density Functional Theory (Springer-Verlag, 2006).
[22] V. Barone, M. Cossi, J. Phys. Chem. A **102**, 1995 (1998); J. Tomasi, B. Mennucci, R. Cammi, Chem. Rev. **105**, 2999 (2005).
[23] Gaussian 03, Revision C.02, M. J. Frisch, G. W. Trucks, H. B. Schlegel, G. E. Scuseria, M. A. Robb, J. R. Cheeseman, J. A. Montgomery Jr., T. Vreven, K. N. Kudin, J. C. Burant, J. M. Millam, S. S. Iyengar, J. Tomasi, V. Barone, B. Mennucci, M. Cossi, G. Scalmani, N. Rega, G. A. Petersson, H. Nakatsuji, M. Hada, M. Ehara, K. Toyota, R. Fukuda, J. Hasegawa, M. Ishida, T. Nakajima, Y. Honda, O. Kitao, H. Nakai, M. Klene, X. Li, J. E. Knox, H. P. Hratchian, J. B. Cross, V. Bakken, C. Adamo, J. Jaramillo, R. Gomperts, R. E. Stratmann, O. Yazyev, A. J. Austin, R. Cammi, C. Pomelli, J. W. Ochterski, P. Y. Ayala, K. Morokuma, G. A. Voth, P. Salvador, J. J. Dannenberg, V. G. Zakrzewski, S. Dapprich, A. D. Daniels, M. C. Strain, O. Farkas, D. K. Malick, A. D. Rabuck, K. Raghavachari, J. B. Foresman, J. V. Ortiz, Q. Cui, A. G. Baboul, S. Clifford, J. Cioslowski, B. B. Stefanov, G. Liu, A. Liashenko, P. Piskorz, I. Komaromi, R. L. Martin, D. J. Fox, T. Keith, M. A. Al-Laham, C. Y. Peng, A. Nanayakkara, M. Challacombe, P. M. W. Gill, B. Johnson, W. Chen, M. W. Wong, C. Gonzalez, J. A. Pople, Gaussian, Inc., Wallingford CT, 2004.
[24] A. Streitwieser, C.H. Heathcock, Introduction to Organic Chemistry, 3rd Edition, Macmillan Publishing Company, New York, 1985.
[25] W.M. Campbell, A.K. Burrell, D.L. Officer, K.W. Jolley, Coord. Chem. Rev. **248**, 1363 (2004).
[26] S. Ruhle, M. Greenshtein, S.-G. Chen, A. Merson, H. Pizem, C.S. Sukenik, D. Cahen, A. Zaban, J. Phys. Chem. B **109**, 18907 (2005).
[27] L.M. Peter, J. Phys. Chem. C **111**, 6601 (2007).
[28] M. K. Nazeeruddin, F. De Angelis, S. Fantacci, A. Selloni, G. Viscardi, P. Liska, S. Ito, T. Bessho, M. Gratzel, J. Am. Chem. Soc. **2005**, 127, 16835.
[29] G. Redmond, D. Fitzmaurice, J. Phys. Chem. **97**, 1426 (1993); S. G. Yan, J. T. Hupp, J. Phys. Chem. **100**, 6867 (1996); M.K. Nazeeruddin, R. Humphry-Baker, P. Liska, M. Gratzel J. Phys. Chem. B 107, 8981 (2003); C.-Y. Chen, H.-C. Lu, C.-G. Wu, J.-G. Chen, K.-C. Ho, Adv. Funct. Mater. **17**, 29 (2007); S. Ruhle, M. Greenshtein, S.-G. Chen, A. Merson, H. Pizem, C.S. Sukenik, D. Cahen, A. Zaban, J. Phys. Chem. B **109**, 18907 (2005).

*Corresponding author: girtu@univ-ovidius.ro